

Identification of key genes in hepatocellular carcinoma and validation of the candidate gene, *cdc25a*, using gene set enrichment analysis, meta-analysis and cross-species comparison

XIAOXU LU^{1*}, WEN SUN^{1*}, YANPING TANG^{1*}, LINGQUN ZHU¹, YUAN LI¹, CHAO OU¹,
CHUN YANG¹, JIANJIA SU¹, CHENGPiao LUO¹, YANLING HU² and JI CAO¹

¹Department of Research, Affiliated Tumor Hospital of Guangxi Medical University, Nanning, Guangxi 530021;

²The Medical Scientific Research Center, Guangxi Medical University, Nanning, Guangxi 530022, P.R. China

Received December 11, 2014; Accepted October 26, 2015

DOI: 10.3892/mmr.2015.4646

Abstract. The aim of the present study was to determine key pathways and genes involved in the pathogenesis of hepatocellular carcinoma (HCC) through bioinformatic analyses of HCC microarray data based on cross-species comparison. Microarray data of gene expression in HCC in different species were analyzed using gene set enrichment analysis (GSEA) and meta-analysis. Reverse transcription-quantitative polymerase chain reaction and western blotting were performed to determine the mRNA and protein expression levels of *cdc25a*, one of the identified candidate genes, in human, rat and tree shrew samples. The cell cycle pathway had the largest overlap between the GSEA and meta-analysis. Meta-analyses showed that 25 genes, including *cdc25a*, in the cell cycle pathway were differentially expressed. *Cdc25a* mRNA levels in HCC tissues were higher than those in normal liver tissues in humans, rats and tree shrews, and the expression level of *cdc25a* in HCC tissues was higher than in corresponding paraneoplastic tissues in humans and rats. In human HCC tissues, the *cdc25a* mRNA level was significantly correlated with clinical stage, portal vein tumor thrombosis and extrahepatic metastasis. Western blotting showed that, *cdc25a* protein levels were significantly upregulated in HCC tissues in humans, rats and tree shrews. In conclusion, GSEA and meta-analysis can be combined to identify key molecules and pathways involved in HCC. This study demonstrated that the cell cycle pathway and the *cdc25a* gene may be crucial in the pathogenesis and progression of HCC.

Introduction

Hepatocellular carcinoma (HCC) is one of the most common types of malignancy worldwide (1). It is associated with a poor prognosis in advanced stages. Identifying therapeutic targets for the treatment of HCC is important. During tumor development, somatically acquired "passenger" mutations owing to the inherent genomic instability of cancer cells, gene linkage, and spontaneous mutagenesis may not confer a selective advantage to the developing tumor (2). Currently, one of the challenges in cancer research is identifying key molecular changes among all acquired "passenger" mutations that promote the formation and development of the tumor. In recent years, genome sequencing projects have been completed in a number of animals, including humans, rats and mice, and genes have been identified that have the same expression in different species indicating that these genes could have conservative and important functions. The strategy of cross-species comparative oncogenomics was developed based on this understanding. Mattison *et al* (3) adopted cross-species comparative genomic hybridization to search for genes that were co-expressed in HCC tissues collected from humans, mice and rats, in order to identify novel candidate genes. The authors of the present study hypothesized that a search for genetic regulators common to humans and other animals, during HCC formation may aid in identifying key genes that affect the pathogenesis and progression of HCC. Gene microarrays have been widely used in HCC research. Analyses on whole-genome mRNA expression microarrays can aid in predicting transcripts that affect the prognosis and recurrence of HCC. However, identifying specific genetic markers that can be used as treatment targets remains a challenge. Mootha *et al* (4) developed GSEA, with which disease-associated gene pathways can be identified at the genomic level using case-control data. In GSEA, gene expression hybridization data in two biological conditions are analyzed to determine a pattern of gene expression in specific functional gene sets and whether such a pattern is statistically significant. In addition, due to differences in experimental platforms, samples, standardization methods and analytical methods, microarray data

Correspondence to: Professor Ji Cao, Department of Research, Affiliated Tumor Hospital of Guangxi Medical University, 71 Hedi Road, Nanning, Guangxi 530021, P.R. China
E-mail: caojicn@163.com

*Contributed equally

Key words: gene set enrichment analysis, meta-analysis, cross-species, *cdc25a*, hepatocellular carcinoma

obtained in different laboratories may differ. Meta-analysis can be a viable solution to this problem, as it can be used to collect and quantitatively analyze data published on the same subject in an integrative manner, thus obtaining more accurate or a larger number of results than can be gained from any individual study (5). In the present study, GSEA and meta-analysis were combined to analyze whole genome and microarray data from five HCC data sets.

Materials and methods

Databases. A systematic literature and database search was performed to identify the HCC-related gene expression profiles of humans and other animals. Relevant data were downloaded from the Gene Expression Omnibus (GEO) database (<http://www.ncbi.nlm.nih.gov/geo/>). The keyword used for the search was 'hepatocellular carcinoma' and the research type was set as expression profiling by array. A total of 230 studies have published gene microarray data. The data sets that met the following criteria were included in this study: The data set must contain whole-genome mRNA expression microarray data; data included a comparison between HCC and normal tissues; both standardized and raw data sets were examined; and the data set had to include >3 samples. Using the above criteria, only five data sets (6-10) were included in the present study (Table I). GSEA and meta-analysis were combined to analyze whole genome and microarray data of these five HCC data sets. The genes that showed significantly differential expression were compared with the mRNA microarray results of a study conducted by our group using the tree shrew HCC model (11) to identify genes in HCC tissue that showed specific changes in >2 species (including humans).

Sample collection.

Human liver tissue samples. All patients have provided written informed consent to have their tissues stored and used for future research. The ethics committee of The Affiliated Tumor Hospital of Guangxi Medical University (Guangxi, China) approved this study. A total of 38 HCC tissue samples and corresponding paraneoplastic tissue samples (>2 cm away from the edge of the tumor) were obtained from patients (age, 24-70 years; mean age, 49.5±11.7) who underwent surgical resection at the Affiliated Tumor Hospital of Guangxi Medical University between January 2009 and December 2011. The diagnosis of HCC in each patient was confirmed histopathologically. Variables including tumor stage, presence of portal vein tumor thrombosis, number and size of tumors, serum α -fetoprotein, tumor differentiation and presence of extrahepatic metastases and recurrence were evaluated in the patients with HCC. The tumor stage was determined according to the Barcelona-Clinic Liver Cancer staging classification (12). Tumor differentiation was graded according to the Edmondson grading system (12). Prior to surgical resection, none of the patients with HCC received chemotherapy. In addition, ten normal liver tissue samples surgically resected from patients with benign liver lesions were also collected.

Rat and tree shrew liver tissue samples. Animal experiments were conducted in accordance with the guidelines for The Care and Use of Laboratory Animals issued by the Ethics Committee of the Affiliated Tumor Hospital of Guangxi Medical

University. Rat and tree shrew animal models of HCC induced by aflatoxin B1 (AFB1) have been previously established by our group (13,14). A total of 42 female Wistar rats (age, 4 weeks; weight, 180-210 g) were housed individually under controlled light (12 h light/dark cycle) and temperature conditions. Food and water were available *ad libitum*. The rats were randomly divided into two groups: An AFB1 group ($n=28$) and a control group ($n=14$). The rats in the AFB1 group were intraperitoneally injected with AFB1 (100-200 μ g/kg) 1-3 times/week. Liver biopsies were obtained from all rats during the 14 th, 28 th, 42 nd and 55 th week, and all rats were sacrificed on the 64 th week by cervical dislocation. A total of 15 HCC tissue samples and 15 corresponding paraneoplastic tissues samples were collected from the rats in the AFB1 group. A total of 14 normal liver tissue samples were collected from the rats in the control group. Adult tree shrews ($n=27$; age, 6 months; weight, 100-160 g) were obtained from the Kunming Institute of Zoology, Chinese Science Academy (Yunnan, China), and were allowed to acclimatize for one week to the facilities prior to the experiment. The tree shrews were housed in individual, suspended, stainless steel wire cages, under controlled environmental conditions with a 12 h light/dark photoperiod. They had *ad libitum* access to tap water and a natural diet containing rice powder (20%), corn powder (20%), beef (20%), wheat bran (10%), soy bean (10%), egg (10%), whole milk powder (5%), and a sugar, salt, vitamin, mineral mix (5%). They were also fed daily with reconstituted powdered milk and fruit. The shrews were randomly divided into an AFB1 group ($n=15$; 9 males and 6 females) and a control group ($n=12$; 6 males and 6 females), and as previously reported (15), the animals in the AFB1 group were fed AFB1 (400 mg/kg body weight/day in a small amount of milk; Sigma-Aldrich, St. Louis, MO, USA) from the 1 st to the 90 th week of the experiment, whereas the animals in control group were raised without AFB1 administration. Liver biopsies from each animal were obtained every three months under Ketamine Hydrochloride anesthesia (50 mg/kg; Fujian Gutian Pharmaceutical Co., Ltd., Fujian, China). In the present study, 10 HCC tissue samples and 10 corresponding paraneoplastic tissue samples were obtained when the animals developed cancer (HCC appeared at the 105 th week of experimentation) following sacrifice by cervical dislocation. A total of 10 normal liver tissue samples were collected from tree shrews in control group. After surgical resection, all tissue samples were subjected to rapid freezing in liquid nitrogen and then stored at -80°C. HCC samples were confirmed histopathologically.

GSEA and meta-analysis. Bioconductor (16) 2.10.1 was used to standardize the data. The Robust Multi-array Average (RMA) algorithm (17,18) in the software package, Affy, was used for background correction, standardization and Log2 conversion of raw data on the Affymetrix platform. A t-test was performed to evaluate each probe in each data set. Only genes that were included in the Kyoto Encyclopedia of Genes and Genomes (KEGG) database (19) were subjected to GSEA. Genes with an interquartile range (IQR) <0.5 were excluded. If one gene corresponded to several probes, only the probe with the highest IQR was used. GSEA was performed using the Category package in Bioconductor. The gene sets represented by ≥ 10 genes were subjected to further analyses, and genes in each pathway were subjected to a

Table I. Basic information on the five whole-genome data sets.

| Data set | Authors, (ref.) | Microarray platform | Experimental design | Number of probes | Species | Sample (n) | Control (n) |
|----------|-------------------------------|---------------------|-------------------------|------------------|---------------------|------------|-------------|
| GSE19665 | Deng <i>et al</i> (6) | U133 Plus 2.0 | Paired tissues | 54000 | <i>Homo sapiens</i> | 10 | 10 |
| GSE9809 | Liao <i>et al</i> (7) | Mouse430_2 | Unpaired+paired tissues | 45000 | <i>Mus musculus</i> | 3 | 7 |
| GSE9012 | Khetchoumian <i>et al</i> (8) | Mouse430_2 | Unpaired tissues | 45000 | <i>Mus musculus</i> | 5 | 5 |
| GSE19004 | Viatour <i>et al</i> (9) | Mouse430_2 | Unpaired tissues | 45000 | <i>Mus musculus</i> | 5 | 4 |
| GSE2127 | Sheth <i>et al</i> (10) | moe430a | Paired tissues | 22000 | <i>Mus musculus</i> | 9 | 6 |

Paired, control for the HCC group came from the same HCC individuals; unpaired, control for the HCC group came from normal individuals.

t-test. After 1,000 permutations, the P-value of each pathway was obtained. The upregulated and downregulated pathways in all five data sets were compared. The cell cycle pathway was upregulated in all five data sets. All genes in the cell cycle pathway were subjected to meta-analysis in each data set. T-tests were conducted using SAS9.13 software (Cary, NC, USA) to calculate the P-value of each probe in the cell cycle pathway in each data set and the χ^2 value of each gene was calculated using the following formula:

$$(LS = \frac{\sum_{i=1}^N (-\log(p_i))}{N})$$

In which the degree of freedom is two times that of the data set K). Genes with $P < 0.05$ were obtained. Analyses on these gene pathways were performed using the Database for Annotation, Visualization and Integrated Discover (DAVID; <http://david.abcc.ncifcrf.gov/>) in KEGG.

Reverse transcription-quantitative polymerase chain reaction (RT-qPCR). Total RNA was extracted from tissue samples using TRIzol reagent (Invitrogen; Thermo Fisher Scientific, Waltham, MA, USA), and first-strand cDNA was synthesized by reverse transcription from 1 μ g RNA using a RevertAid First Strand cDNA Synthesis kit (Thermo Fisher Scientific, Inc.). RT-qPCR was performed using a standard protocol from the SYBR[®] Premix Ex Taq kit (Takara, Dalian, China) on an Applied Biosystems 7300/7500 Real Time PCR system (Applied Biosystems, Grand Island, NY, USA). The cycling conditions were as follows: 95°C for 30 sec, and 40 cycles at 95°C for 5 sec followed by 60°C for 34 sec. The relative mRNA expression levels of *cdc25a* to control GAPDH were analyzed using ABI PRISM 7300 software v1.3.1 (Applied Biosystems) and calculated with the double standard curves method. The *cdc25a* forward and reverse primer sequences were 5'-CCAAAGGAACCATGAGAAC-3' and 5'-CAGATGCCATAATTTCTGGAG-3', respectively, and the product length was 138 bp. The forward and reverse primer sequences for the internal control gene, 3-phosphate dehydrogenase (GAPDH), were 5'-AAGAAGGTGGTGAAGCAGGC-3' and 5'-ACCACCCTGTTGCTGTAGCC-3', respectively, and the product length was 200 bp.

Western blot analysis. Western blot analysis to assess *cdc25a* and GAPDH expression was performed as previously described (14). Protein samples (60 μ g) were separated by 10% SDS-PAGE,

prior to being transferred onto PVDF membranes (EMD Millipore, Billerica, MA, USA). The membranes were subsequently blocked with Tris-buffered saline with Tween 20 (TBST; Beyotime Institute of Biotechnology, Haimen, China) containing 5% (w/v) skimmed milk powder for c. 2 h at room temperature and then incubated at 4°C overnight with the following primary antibodies: Rabbit polyclonal anti-human Cdc25 (cat. no. ab75743; Abcam, Cambridge, MA, USA) or mouse monoclonal anti-human glyceraldehyde 3-phosphate dehydrogenase (GAPDH; cat. no. TA-08; Beijing Zhongshan Golden Bridge Biotech Co., Ltd., Beijing, China) at dilutions of 1:100 or 1:1000, respectively. The membranes were then washed three times with TBST buffer, and incubated for 1 h at room temperature with IRDye 680LT goat anti-mouse secondary antibody (cat. no. 0926-68020; LI COR Biosciences, Lincoln, NE, USA) or IRDye 680LT goat anti-rabbit secondary antibody (cat. no. 926-68021; LI-COR Biosciences) at 1:7,500 dilution. The membranes were scanned using an Odyssey infrared imaging system (LI-COR Biosciences). Quantification of bands was achieved by ratiometric analysis of the fluorescent intensities of *cdc25a* and GAPDH using Odyssey Application Software 3.0 (LI-COR Biosciences).

Statistical analysis. SPSS 13.0 (SPSS, Inc., Chicago, IL, USA) was used for data analysis. Quantitative data are expressed as the mean \pm standard deviation. Comparison of mean values between multiple groups was performed using a one-way analysis of variance. $P < 0.05$ was considered to indicate a statistically significant difference.

Results

Results of GSEA analysis. GSEA was performed for functional gene enrichment of the five data sets to search for key upregulated and downregulated pathways affecting these data sets. In GSE19665, 27 upregulated and 71 downregulated pathways were enriched; in GSE9809, 56 upregulated and 4 downregulated pathways were enriched; in GSE9012, 66 upregulated and 34 downregulated pathways were enriched; in GSE19004, 73 upregulated and 51 downregulated pathways were enriched; and in GSE2127, 69 upregulated and 50 downregulated pathways were enriched. There was a large amount of overlap between pathways in the GSE19665 and GSE19004 data sets. Downregulated pathways common to all five data sets included the linoleic acid metabolic pathway and the

Table II. Distribution of differentially expressed genes revealed by meta-analyses of five data sets.

| Gene | P-value |
|-----------|----------|
| ABI3BP | 3.23E-06 |
| CCNB1 | 5.37E-06 |
| NEK2 | 7.66E-06 |
| MKI67 | 1.35E-05 |
| cdc20 | 2.46E-05 |
| angptl6 | 2.47E-05 |
| rrm2 | 2.74E-05 |
| Ttc36 | 3.06E-05 |
| UBE2C | 3.18E-05 |
| mcm2 | 4.07E-05 |
| ASPM | 4.29E-05 |
| NCAPH | 5.23E-05 |
| TUBA1B | 5.23E-05 |
| CCNB2 | 5.45E-05 |
| Hist1h2ad | 5.71E-05 |
| TOP2A | 5.91E-05 |
| FOXM1 | 6.58E-05 |
| BIRC5 | 7.18E-05 |
| STMN1 | 7.74E-05 |
| racgap1 | 7.84E-05 |
| Hist1h2ag | 7.94E-05 |
| Hist1h2ah | 7.94E-05 |
| Hist1h2ai | 7.94E-05 |
| CDCA5 | 9.89E-05 |

arachidonic acid metabolic pathway. Upregulated pathways common to all five data sets included the amino sugar and nucleotide sugar metabolic pathways, the cell cycle pathway and the thyroid cancer pathway.

Results of meta-analysis. A total of 220 positive genes were found in the GSE19665 data set and 213 positive genes were found in the remaining four data sets. After the P-value of each gene was obtained, SAS13.0 software was used for meta-analysis. A total of 1,708 genes were found to have $P < 0.05$ and 24 genes were found to have $P < 10^{-4}$ (Table II).

The 1,708 genes were subjected to pathway enrichment using the DAVID KEGG database. A total of 720 of these genes were found in the KEGG database.

Overlapping results obtained with GSEA and meta-analysis. The cell cycle pathway had the largest overlap between the GSEA and meta-analysis. Gene probe numbers in the cell cycle pathway of the five data sets were obtained using R programming language. The probe numbers were sent to the website, <http://david.abcc.ncifcrf.gov/conversion.jsp>, to obtain the official names of the genes. There were 99 differentially expressed genes in the cell cycle pathway of data set GSE19665, 96 in GSE9809, 90 in GSE9012, 106 in GSE19004 and 113 in GSE2127. Meta-analyses demonstrated that 25 genes involved in the cell cycle pathway were differentially

Table III. Distribution of differentially expressed genes in the cell cycle pathway.

| Gene | χ^2 value | P-value |
|--------|----------------|----------|
| CCNB2 | 46.94 | 9.67E-07 |
| mcm2 | 36.51 | 6.89E-05 |
| YWHAB | 35.63 | 9.74E-05 |
| CCNA2 | 33.83 | 2.00E-04 |
| CDKN2C | 32.60 | 3.00E-04 |
| Cdk1 | 32.24 | 4.00E-04 |
| MCM6 | 32.07 | 4.00E-04 |
| cdkn2b | 30.15 | 8.00E-04 |
| CCNB1 | 30.15 | 8.00E-04 |
| CDC25A | 29.98 | 9.00E-04 |
| Mad211 | 29.43 | 1.10E-03 |
| MCM7 | 28.57 | 1.50E-03 |
| CCNE1 | 28.21 | 1.70E-03 |
| MCM4 | 46.94 | 3.00E-03 |
| cdc20 | 36.51 | 6.50E-03 |
| smc3 | 35.63 | 6.70E-03 |
| pcnA | 33.83 | 7.90E-03 |
| RAD21 | 32.60 | 9.00E-03 |
| CDKN1A | 32.24 | 9.60E-03 |
| CCND1 | 32.07 | 1.08E-02 |
| SMAD3 | 30.15 | 1.16E-02 |
| TGFB1 | 30.15 | 1.27E-02 |
| YWHAZ | 29.98 | 2.06E-02 |
| YWHAG | 29.43 | 2.08E-02 |
| YWHAH | 28.57 | 2.52E-02 |

expressed ($P < 0.05$). The names, χ^2 values and P-values of these genes are shown in Table III.

Cdc25a mRNA expression. The results of the present study identified 25 differential expression genes in the cell cycle signaling pathway, as determined by GSEA and meta-analysis which analyzed five data sets from human HCC tissue samples. Among the 25 candidate genes, Cdc25a was also shown to be overexpressed in the HCC tissue samples of diethylnitrosamine-induced rats and aflatoxin B1-induced tree shrews (11,20). Therefore, Cdc25a mRNA expression was further investigated. Results of real-time fluorescent PCR showed that the cdc25a mRNA expression level in human HCC tissue (0.00425 ± 0.00241) was significantly higher than in the corresponding paraneoplastic tissue (0.00086 ± 0.00081) ($P < 0.05$) and in normal liver tissue (0.00038 ± 0.00032) ($P < 0.05$). There was no significant difference between the paraneoplastic tissue and normal liver tissue ($P > 0.05$). The cdc25a mRNA expression level in rat HCC tissue (0.00281 ± 0.00278) was significantly higher than that in the corresponding paraneoplastic tissue (0.00044 ± 0.00035) ($P < 0.05$) and in normal liver tissue (0.00051 ± 0.00022) ($P < 0.05$); however, there was no significant difference between the paraneoplastic tissue and normal liver tissue ($P > 0.05$). The cdc25a mRNA expression level in tree shrew HCC

Table IV. Correlation between the detection rate of *cdc25a* mRNA in human HCC tissues and clinical parameters.

| Clinical parameter | n | Cdc25a mRNA expression level | t-value | P-value |
|--------------------------------------------|----|------------------------------|---------|---------|
| BCLC stage (12) | | | | |
| 0, A | 26 | 0.00253±0.00175 | 2.342 | 0.023 |
| B, C | 12 | 0.00537±0.00221 | | |
| PVTT | | | | |
| Yes | 10 | 0.00564±0.00259 | 0.505 | 0.030 |
| No | 28 | 0.00376±0.00214 | | |
| Extrahepatic metastasis | | | | |
| Yes | 11 | 0.00571±0.00254 | 0.139 | 0.014 |
| No | 27 | 0.00367±0.00208 | | |
| Recurrence | | | | |
| Yes | 20 | 0.00408±0.00250 | 0.071 | 0.632 |
| No | 18 | 0.00446±0.00229 | | |
| Tumor diameter (cm) | | | | |
| ≥5 | 31 | 0.00436±0.00236 | 0.218 | 0.568 |
| <5 | 7 | 0.00378±0.00262 | | |
| Number of tumors | | | | |
| 1 | 24 | 0.00375±0.00203 | 1.886 | 0.083 |
| ≥2 | 14 | 0.00513±0.00274 | | |
| Serum AFP (μg/l) | | | | |
| ≥400 | 13 | 0.00521±0.00249 | 0.215 | 0.075 |
| <400 | 25 | 0.00376±0.00221 | | |
| Tumor differentiation | | | | |
| Highly differentiated | 21 | 0.00434±0.00217 | 1.602 | 0.825 |
| Poorly differentiated and undifferentiated | 17 | 0.00416±0.00268 | | |

BCLC, Barcelona Clinic Liver Cancer; PVTT, portal vein tumor thrombus; AFP, α-fetoprotein.

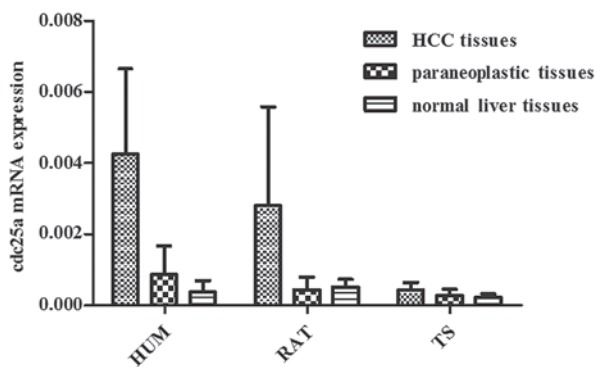


Figure 1. Expression of *cdc25a* mRNA in the HCC, paraneoplastic and normal liver tissues of different species (humans, rats and tree shrews). HUM, human; RAT, rat; TS, tree shrew.

tissue (0.00043±0.00021) was significantly higher than that in normal liver tissue (0.00022±0.00010) ($P<0.05$), however there was no significant difference between the paraneoplastic tissue (0.00028±0.00017) and corresponding HCC tissue or normal liver tissue ($P>0.05$; Fig. 1).

The 38 HCC patients were grouped on the basis of whether they had PVTT, extrahepatic metastasis, BCLC stage,

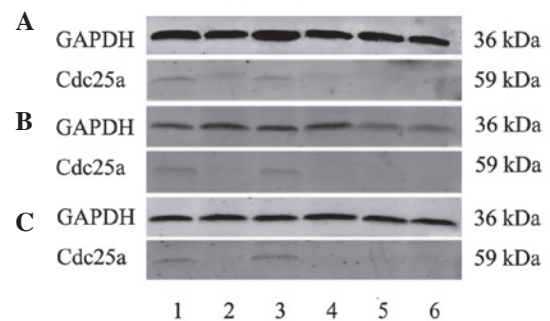


Figure 2. Cdc25a protein expression in the HCC, paraneoplastic and normal liver tissues of different species (humans, rats and tree shrews), revealed by western blot analysis. (A) *cdc25a* protein expression in human liver tissues; (B) *cdc25a* protein expression in rat liver tissues; and (C) *cdc25a* protein expression in tree shrew liver tissues. Lanes 1 and 3, HCC tissue; lanes 2 and 4, corresponding paraneoplastic tissue; and lanes 5 and 6, normal liver tissue. GAPDH, 3-glyceraldehyde phosphate dehydrogenase.

postoperative recurrence, tumor diameter, number of tumors, serum AFP level and degree of tumor differentiation. The correlation between *cdc25a* mRNA expression in the HCC tissues and the above clinical parameters was examined. As demonstrated in Table IV, the detection rate of *cdc25a* mRNA

was observed to be significantly correlated with Barcelona Clinic Liver Cancer (BCLC) stage, portal vein tumor thrombus (PVTT) and extrahepatic metastasis, but not with postoperative recurrence, tumor diameter, tumor number, serum α -fetoprotein (AFP) level or degree of tumor differentiation.

Cdc25a protein expression. Based on the results of fluorescent quantitative PCR, 38 human HCC and corresponding paraneoplastic tissue samples, 10 normal human liver tissue samples, 15 rat HCC and corresponding paraneoplastic tissue samples, 10 normal rat liver tissues, 10 tree shrew HCC and corresponding paraneoplastic tissue samples, and 10 normal tree shrew liver tissue samples were collected for western blot analysis. Specific *cdc25a* and GAPDH protein bands were observed at 36 and 59 kDa of pre-stained proteins, respectively, although the target protein, *cdc25a*, was not detected in normal human liver tissue, or in the normal or paraneoplastic liver tissues of rats or tree shrews. The mean relative *cdc25a* expression level in human HCC tissues (0.339 ± 0.239) was significantly higher than in the corresponding paraneoplastic tissues (0.0609 ± 0.0498 ; $P < 0.05$). In humans, rats and tree shrews, the *cdc25a* bands were notably stronger in HCC tissues than in the corresponding paraneoplastic and normal liver tissues, consistent with the high *cdc25a* mRNA expression in HCC tissues (Fig. 2).

Discussion

Analyses on gene microarray data are an important part of gene microarray research. A lot of useful information may be missed due to potential problems with the samples when analyzing the results of a single experiment. In addition, using a t-test to target a single set of microarray data has certain limitations. The small sample size may lead to an unreliable variance estimation, resulting in a high false-positive rate, whereas differences in the expression levels of different samples may be ignored (21). In GSEA, microarray data of samples in two different biological states (e.g., normal vs. cancerous) are analyzed to determine whether a set of genes show similar expression trends between the two states, thereby identifying genes or pathways associated with the disease (22).

In the present study, GSEA and meta-analysis were combined to analyze five data sets, and the two results were compared in order to identify HCC-related genes and pathways. DEGs in >2 groups of samples were analyzed using GSEA and the clustering was performed using differentially expressed genes. R programming language was used to process the data and for statistical analysis to obtain pathways that showed changes common to all five data sets. DEGs were analyzed using the DAVID website to determine the pathways in which these genes may be involved. The cell cycle pathway statistically significant in the results obtained with the GSEA and meta-analysis and was further analyzed to identify genes with significant differential expression.

Among the 25 differentially expressed genes in the cell cycle pathway that were identified, cyclin B2, cyclin B1, cyclin D1, *cdc25a* and *cdk1* are closely associated with HCC occurrence and development (23-26). Cyclin-dependent kinases (CDKs) are core proteins in the cell cycle regulatory network. Changes in the expression activity of CDKs directly affect the length of the cell cycle, determine the progression

of the cell cycle, and are closely associated with the growth, differentiation, migration and apoptosis of normal cells, as well as the occurrence, development and metastasis of tumors (27). CDKs are important in the regulation of hepatoma cell proliferation and apoptosis. Cyclin B and cyclin D are members of the cyclin family and determine which CDKs phosphorylate which substrates as well as when and where. Studies have shown that (27) Cyclin D1 is expressed in normal liver tissue, but its expression is increased in HCC tissue, and is correlated with the histological grade of HCC. This suggests that Cyclin D1 is involved in the progression and development of HCC and may promote cell proliferation, contributing to tumor formation. Cyclin B1 is in the same family, is highly expressed in HCC tissue and is key in the transition process of HCC cells. *Cdc25A* is a phosphatase with dual specificity, and can activate CDKs, promoting the progression of the cell cycle.

Studies have shown that *cdc25a* is associated with breast cancer (28), non-small cell lung cancer (29), colorectal cancer (30), prostate cancer (31) and other malignant tumors. However, there are few studies regarding the correlation between *cdc25a* and liver cancer. In a study by Xu *et al* (26), *cdc25a* expression was examined in HCC tissues using RT-PCR, immunohistochemistry and western blotting, and reported *cdc25a* expression detection rates of 69 (9/13), 56 (33/59) and 78% (46/59), respectively. Immunohistochemistry tests showed that high *cdc25a* protein expression was positively correlated with poor tumor differentiation and PVTT. In the present study, fluorescent quantitative PCR and western blotting showed that *cdc25a* expression was high in human HCC tissues at the transcriptional and at the translational levels. The *cdc25a* mRNA expression level in human HCC tissues was found to be positively correlated with PVTT and extrahepatic metastasis. This suggests that *cdc25a* is associated with the progression of HCC, and may serve as an indicator to evaluate the severity of the disease. The differences between the results of the present study and those of Xu *et al* (26) may be due to differences in sample sources, transcription and translation levels, and experimental method.

In this study, overexpression of *cdc25a* was also found in HCC samples from aflatoxin B1-induced rat and tree shrew HCC models. Such consistent differential expression in different species has also been reported in a previous study by our group (11). The same cross-species expression patterns suggest that *cdc25a* is key in the pathogenesis and progression of HCC. Xu *et al* (32) explored the possibility of using *cdc25a* as an antitumor target by inhibiting its activity in HCC cell lines. It was reported that antisense oligonucleotides of *cdc25a* inhibited 25-50% of cell growth within 48 h, resulting in arrest at the G0-G1 phase and effectively suppressing the proliferation of HCC cells. This suggests that *cdc25a* can serve as a feasible target for anti-cancer treatment. In addition, a study by Liu *et al* (33) showed that knockdown of the ROCK2 gene could activate the reduced ubiquitin-proteasome pathway, thereby promoting *cdc25a* ubiquitination, which would ultimately lead to *cdc25a* degradation and inhibition of HCC cell growth. Therefore, *cdc25a* may be a novel target for anti-HCC treatment.

In conclusion, GSEA and meta-analysis can be combined to identify key molecules and pathways involved in the

pathogenesis and progression of HCC. The cell cycle pathway and the *cdc25a* gene may be the crucial in the pathogenesis and progression of HCC.

Acknowledgements

The present study was supported by the National Science Foundation of China (grant no. 30960428).

References

- Waly Raphael S, Yangde Z and Yuxiang C: Hepatocellular carcinoma: Focus on different aspects of management. *ISRN Oncol* 2012: 421673, 2012.
- Beroukhi R, Mermel CH, Porter D, Wei G, Raychaudhuri S, Donovan J, Barretina J, Boehm JS, Dobson J, Urashima M, *et al*: The landscape of somatic copy-number alteration across human cancers. *Nature* 463: 899-905, 2010.
- Mattison J, Kool J, Uren AG, de Ridder J, Wessels L, Jonkers J, Bignell GR, Butler A, Rust AG, Brosch M, *et al*: Novel candidate cancer genes identified by a large-scale cross-species comparative oncogenomics approach. *Cancer Res* 70: 883-895, 2010.
- Mootha VK, Lindgren CM, Eriksson KF, Subramanian A, Sihag S, Lehar J, Puigserver P, Carlsson E, Ridderstråle M, Laurila E, *et al*: PGC-1 α -responsive genes involved in oxidative phosphorylation are coordinately downregulated in human diabetes. *Nat Genet* 34: 267-273, 2003.
- Greenbaum D, Jansen R and Gerstein M: Analysis of mRNA expression and protein abundance data: An approach for the comparison of the enrichment of features in the cellular population of proteins and transcripts. *Bioinformatics* 18: 585-596, 2002.
- Deng YB, Nagae G, Midorikawa Y, Yagi K, Tsutsumi S, Yamamoto S, Hasegawa K, Kokudo N, Aburatani H and Kaneda A: Identification of genes preferentially methylated in hepatitis C virus-related hepatocellular carcinoma. *Cancer Sci* 101: 1501-1510, 2010.
- Liao YJ, Liu SP, Lee CM, Yen CH, Chuang PC, Chen CY, Tsai TF, Huang SF, Lee YH and Chen YM: Characterization of a glycine N-methyltransferase gene knockout mouse model for hepatocellular carcinoma: Implications of the gender disparity in liver cancer susceptibility. *Int J Cancer* 124: 816-826, 2009.
- Khetchoumian K, Teletin M, Tisserand J, Mark M, Herquel B, Ignat M, Zucman-Rossi J, Cammas F, Lerouge T, Thibault C, *et al*: Loss of Trim24 (Tif1 α) gene function confers oncogenic activity to retinoic acid receptor α . *Nat Genet* 39: 1500-1506, 2007.
- Viatour P and Sage J: Mouse HCC model. <http://www.ncbi.nlm.nih.gov/geo/query/acc.cgi?acc=GSE19004>. Accessed Jul 28, 2012.
- Sheth SS, Bodnar JS, Ghazalpour A, Thippavong CK, Tsutsumi S, Tward AD, Demant P, Kodama T, Aburatani H and Lusis AJ: Hepatocellular carcinoma in *Txnip*-deficient mice. *Oncogene* 25: 3528-3536, 2006.
- Li Y, Wan DF, Su JJ, Cao J, Ou C, Qiu XK, Ban KC, Yang C, Qin LL, Luo D, *et al*: Differential expression of genes during aflatoxin B(1)-induced hepatocarcinogenesis in tree shrews. *World J Gastroenterol* 10: 497-504, 2004.
- Sobin LH and Compton CC: TNM seventh edition: what's new, what's changed: communication from the International Union Against Cancer and the American Joint Committee on Cancer. *Cancer* 116: 5336-5339, 2010.
- Li Y, Qin X, Cui J, Dai Z, Kang X, Yue H, Zhang Y, Su J, Cao J, Ou C, *et al*: Proteome analysis of aflatoxin B1-induced hepatocarcinogenesis in tree shrew (*Tupaia belangeri chinensis*) and functional identification of candidate protein peroxiredoxin II. *Proteomics* 8: 1490-1501, 2008.
- Hao YR, Yang F, Cao J, Ou C, Zhang JJ, Yang C, Duan XX, Li Y and Su JJ: Ginkgo biloba extracts (EGb761) inhibits aflatoxin B1-induced hepatocarcinogenesis in Wistar rats. *Zhong Yao Cai* 32: 92-96, 2009 (In Chinese).
- Li Y, Su JJ, Qin LL, Egner PA, Wang J, Groopman JD, Kensler TW and Roebuck BD: Reduction of aflatoxin B1 adduct biomarkers by oltipraz in the tree shrew (*Tupaia belangeri chinensis*). *Cancer Lett* 154: 79-83, 2000.
- Gentleman RC, Carey VJ, Bates DM, Bolstad B, Dettling M, Dudoit S, Ellis B, Gautier L, Ge Y, Gentry J, *et al*: Bioconductor: Open software development for computational biology and bioinformatics. *Genome Biol* 5: R80, 2004.
- Irizarry RA, Hobbs B, Collin F, Beazer-Barclay YD, Antonellis KJ, Scherf U and Speed TP: Exploration, normalization, and summaries of high density oligonucleotide array probe level data. *Biostatistics* 4: 249-264, 2003.
- Gautier L, Cope L, Bolstad BM and Irizarry RA: Affy-analysis of affymetrix GeneChip data at the probe level. *Bioinformatics* 20: 307-315, 2004.
- Kanehisa M and Goto S: KEGG: Kyoto encyclopedia of genes and genomes. *Nucleic Acids Res* 28: 27-30, 2000.
- Liang HJ, Wei W, Kang XN, Guo K, Cao J, Su JJ, Yang C, Ou C, Li Y and Liu YK: Differentially expressed proteins in the precancerous stage of rat hepatocarcinogenesis induced by diethylnitrosamine. *Chinese Journal of Hepatology* 17: 669-674, 2009 (In Chinese).
- MacDonald JW and Ghosh D: COPA-cancer outlier profile analysis. *Bioinformatics* 22: 2950-2951, 2006.
- Subramanian A, Kuehn H, Gould J, Tamayo P and Mesirov JP: GSEA-P: A desktop application for gene set enrichment analysis. *Bioinformatics* 23: 3251-3253, 2007.
- Takashima S, Saito H, Takahashi N, Imai K, Kudo S, Atari M, Saito Y, Motoyama S and Minamiya Y: Strong expression of cyclin B2 mRNA correlates with a poor prognosis in patients with non-small cell lung cancer. *Tumour Biol* 35: 4257-4265, 2014.
- Gao SY, Li J, Qu XY, Zhu N and Ji YB: Downregulation of Cdk1 and cyclinB1 expression contributes to oridonin-induced cell cycle arrest at G2/M phase and growth inhibition in SGC-7901 gastric cancer cells. *Asian Pac J Cancer Prev* 15: 6437-6441, 2014.
- Li T, Zhao X, Mo Z, Huang W, Yan H, Ling Z and Ye Y: Formononetin promotes cell cycle arrest via downregulation of Akt/Cyclin D1/CDK4 in human prostate cancer cells. *Cell Physiol Biochem* 34: 1351-1358, 2014.
- Xu X, Yamamoto H, Sakon M, Yasui M, Ngan CY, Fukunaga H, Morita T, Ogawa M, Nagano H, Nakamori S, *et al*: Overexpression of CDC25A phosphatase is associated with hypergrowth activity and poor prognosis of human hepatocellular carcinomas. *Clin Cancer Res* 9: 1764-1772, 2003.
- Liu L, Schwartz B, Tsubota Y, Raines E, Kiyokawa H, Yonekawa K, Harlan JM and Schnapp LM: Cyclin-dependent kinase inhibitors block leukocyte adhesion and migration. *J Immunol* 180: 1808-1817, 2008.
- Brunetto E, Ferrara AM, Rampoldi F, Talarico A, Cin ED, Grassini G, Spagnuolo L, Sassi I, Ferro A, Cuorvo LV, *et al*: CDC25A protein stability represents a previously unrecognized target of HER2 signaling in human breast cancer: Implication for a potential clinical relevance in trastuzumab treatment. *Neoplasia* 15: 579-590, 2013.
- Younis RH, Cao W, Lin R, Xia R, Liu Z, Edelman MJ, Mei Y, Mao L and Ren H: CDC25A (Q110del): A novel cell division cycle 25A isoform aberrantly expressed in non-small cell lung cancer. *PLoS One* 7: e46464, 2012.
- Huang MY, Wang JY, Chang HJ, Kuo CW, Tok TS and Lin SR: CDC25A, VAV1, TP73, BRCA1 and ZAP70 gene overexpression correlates with radiation response in colorectal cancer. *Oncol Rep* 25: 1297-1306, 2011.
- Chiu YT, Han HY, Leung SC, Yuen HF, Chau CW, Guo Z, Qiu Y, Chan KW, Wang X, Wong YC and Ling MT: CDC25A functions as a novel Ar corepressor in prostate cancer cells. *J Mol Biol* 385: 446-456, 2009.
- Xu X, Yamamoto H, Liu G, Ito Y, Ngan CY, Kondo M, Nagano H, Dono K, Sekimoto M and Monden M: CDC25A inhibition suppresses the growth and invasion of human hepatocellular carcinoma cells. *Int J Mol Med* 21: 145-152, 2008.
- Liu T, Yu X, Li G, Yuan R, Wang Q, Tang P, Wu L, Liu X, Peng X and Shao J: Rock2 regulates Cdc25A through ubiquitin proteasome system in hepatocellular carcinoma cells. *Exp Cell Res* 318: 1994-2003, 2012.